



URBAN SEISMIC RESILIENCE PLANNING OF PUBLIC SCHOOL INFRASTRUCTURE IN 2 METRO MANILA CITIES

K. Jeswani⁽¹⁾, J. Guo⁽²⁾, C. Christopoulos⁽³⁾

⁽¹⁾ Graduate Researcher, Department of Civil Engineering, University of Toronto, Toronto, Canada, kevin.jeswani@mail.utoronto.ca

⁽²⁾ Seismic Risk Lead, Kinetica, Toronto, Canada, j.guo@kineticadynamics.com

⁽³⁾ Professor, Department of Civil Engineering, University of Toronto, Toronto, Canada, c.christopoulos@utoronto.ca

...

Abstract

This paper presents an integrated seismic resilience evaluation for the public school building infrastructure in Makati (MC) and Quezon City (QC), Metro Manila, Philippines. The full portfolio consists of 1,028 spatially distributed public school buildings that provide education infrastructure for approximately 500,000 students. The data collection process involved rapid visual screening (RVS) conducted in early 2018 on a total of 128 buildings (55% and 14% of the MC and QC portfolio, respectively) following the FEMAP-154 Methodology to enhance the cities' existing high-level building inventory. The buildings, which are primarily low- and mid-rise ductile/non-ductile reinforced concrete moment frames, were categorized into archetypes based on seismic force resisting systems, code vintage, and irregularities. The archetype definitions were based on existing drawings, while structural re-designs were carried out using the applicable code vintages when as-built drawings were not available. Intensity-based seismic performance assessment is applied to the portfolio following the approach outlined in the FEMA P-58 and the REDi guidelines using collapse fragility and vulnerability data generated from non-linear time-history analysis for the primary building archetypes. A seismic risk evaluation was conducted with decision-variables derived from these models. Using this decision-support framework, portfolio-level risk mitigation strategies that consider multiple performance goals are also explored.

Keywords: performance-based seismic risk assessment; school building portfolio analysis; REDi; FEMA P-58; RVS



1. Introduction

The Philippines, situated in the tectonically active region between Philippine Sea Plate and the Sunda Plate [1] recently experienced an earthquake swarm. M_s 6.3 to 6.9, near the southern regional capital of Davao City between October 16 to December 15, 2019, resulting in the temporary and long-term functional loss of over 1,800 schools and the disruption of 3.4 million [2] Metro Manila (*MM*), the capital of the Philippines with a population over 13 million, is transected by the West (*WVF*) and East Valley Fault (*EVF*). Studies (*MMEIRS* & *GMMA-RAP*) on the regional seismic risk in *MM* [3;4] have shown that the tectonic setting of the *MM* poses a significant threat, suggesting that in the range of M_w 7.2 to 7.5 can be produced by the *WVF* and *EVF* respectively, and have a return period less than 500 years, suggesting that the tectonic activity is due given that the last significant event by the two faults is speculated to have been in 1658.

Regional *MM* seismic risk studies [3;4] and a study on the seismic-hazard prioritization of all public schools in *MM* [5] take a macroscopic risk approaches, using *HAZUS* [6], due its ability to provide rapid loss estimation of very large building portfolios. In contrast to the use of *HAZUS*-type single-degree-of-freedom (*SDOF*) systems representative of general building archetypes, the implementation of building-specific probabilistic earthquake risk assessments with *FEMA P-58* [7] or the *USRC* [8] rating system methodologies incorporate non-linear dynamic time-history (*NLDTH*) analysis results. Macroscopic approaches do not capture enough resolution for specific risk mitigation strategies for owners of relatively large building portfolios (in the tens to hundreds). While building-specific methods may offer financial and safety risk management decision support tools backed by quantitative means, they may not be financially feasible and time efficient. Arup [9] incorporate a “hybrid” approach using sophisticated *NLDTH* models capturing the fragility and/or vulnerability functions of buildings in a portfolio. The *FEMA P-58* methodology is used for building-specific risk analyses to characterize vulnerability functions and for a direct *NLDTH*-based portfolio analysis. They implement their *REDi* downtime assessment methodology [10], in an ongoing project to improve the seismic resilience of a 328-building portfolio at the University of British Columbia. Rapid Visual Screening (*RVS*) following *FEMAP-154* [11], detailed 3D *NLDTH* with intensity-based analyses. building component losses (using *FEMA P-58*) and downtime estimates (using *REDi*) for each realization of a specific earthquake scenario. *FEMAP-154* scores were used to confirm quantitative collapse risk assessments developed from the non-linear *MDOF* models.

Following the methodology outlined in a preliminary study [12], this paper presents an update on the research into a similar hybrid seismic risk analysis framework to assess the seismic resilience of a spatially distributed building portfolio of 1,028 public school buildings with approximately 500,000 students across two cities in *MM*. The data collection process involved *RVS* conducted in early 2018 on a total of 128 buildings following *FEMAP-154* assess available building inventories and to allow for extrapolation in classifying the structural systems of the remaining buildings. The buildings were categorized using the typologies established by the University of the Philippines (*UPD-ICE*) [13] with taxonomy based on *HAZUS*. Detailed 3D non-linear models are developed for four of the primary archetypes, which are low- to mid-rise ductile/non-ductile reinforced concrete moment frames (*RC-MRFs*) for a preliminary portfolio loss estimation exercise. The archetype definitions were based on existing drawings, while structural re-designs were carried out using the applicable code vintages when drawings were not available. To appropriately assemble a ground-motion (*GM*) suites for *NLDTH*, seismic hazards were defined based on the latest Philippine Earthquake Model [1]. Careful consideration to near-fault effects were made and a spectral-matching procedure of global *GM* suites was undertaken. *FEMA P-58* and the *REDi* guidelines using vulnerability data generated from non-linear time-history analysis of detailed 3D models of primary building archetypes. *FEMAP-154* screening and scoring for collapse evaluation, *FEMA P-58* for non-collapse losses, and the *REDi* methodology for the non-collapse downtime estimation (re-occupancy, functional recovery and full recovery times). Finally, the reduced portfolio (only 4 archetypes) is evaluated with 1 of the 18 seismic scenarios presented in the *MMEIRS* [4] study, representing the greatest hazard for *MM*.



2. Proposed Portfolio Risk Methodology

Building-specific risk assessments following the *FEMA P-58* methodology utilizes seismic intensity measures (*IM*, e.g. spectral acceleration at the building fundamental period, $S_a(T)$) to generate *EDPs* and to determine component damage states (*DS*), providing the end-user with consequences or decision-variables (*DVs*) to make informed decisions about a building portfolio. The generation of *EDPs* for given *IMs* is often the most time-consuming task in this exercise, however in the case of building portfolios comprised of similar structures, the use of a few representative buildings to model the loss of a much larger building portfolio can exhibit a balance between computational effort and accuracy. The hybrid approach outlined herein takes advantage of the higher resolution of loss data offered by the building-specific analysis for only for a small fraction of the buildings, which can be completely separated from the rest of the portfolio analysis.

Fig. 1a) summarizes the key steps in the proposed methodology for portfolio seismic risk analysis. The proposed procedure starts with the classification and identification of key representative buildings within the portfolio used to derive loss distributions. For archetype identified, a building-specific loss analysis is performed using *NLDTH* analyses over an entire range of possible seismic intensities to extract *EDPs*. Losses (ie. financial, *REDi* recovery time, and casualties) are derived from *EDPs* and constructing the loss distribution curves conditioned on the current seismic intensity. The improvements of the proposed method relate to the generalization of the loss distributions to capture consequences other than financial loss, and in the method for constructing the loss distribution curves. The resulting loss distributions contain all the necessary information for portfolio loss simulation and are assigned to each building in the portfolio.

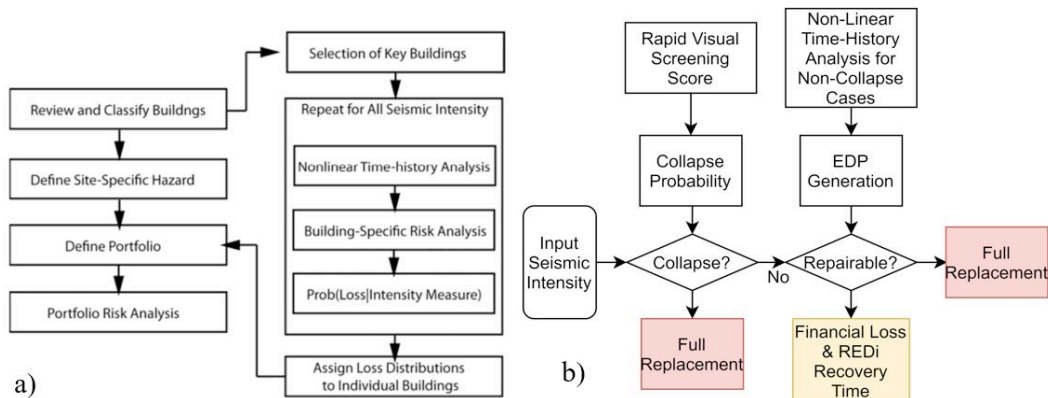


Fig. 1 – Portfolio analysis using building-specific loss distributions of key archetypes

Portfolio risk analyses are performed using Monte Carlos Simulations, in which losses shown in Eq. (1) are calculated repeatedly for a fixed number of realizations:

$$L^{[k]}_{ij} = F^{-1}(p^{[k]}_{ij} | IM = im_{ij}) \quad (1)$$

where $L^{[k]}$ is the k^{th} consequence in the loss vector for a specific site, where k = financial loss, REDI reoccupancy time, functional recovery time, and full recovery time. The term $L^{[k]}_{ij}$ denotes the k^{th} consequence for the i^{th} site in the j^{th} realization. The function F is the conditional probability distribution for losses given the seismic input intensity, which are derived from the building-specific loss analysis of corresponding key buildings in the portfolio using the multiple stripes method [14] where the loss distributions are computed at discretized intensity levels. The inverse of the conditional loss distribution F^{-1} maps a given probability of non-exceedance, $p^{[k]}_{ij}$ and an input intensity, im_{ij} to the loss value. During each realization, an intensity measure is generated for each building site in the portfolio in accordance with the hazard model. A scenario-based portfolio analysis is examined in this paper, in which stochastic events can be generated using appropriate ground-motion prediction equations



(*GMPEs*) and correlation models, resulting in *IMs* intensity measure is determined at each site, with a random sampling of probability uniquely determining the loss. In this manner, ultimate *DVs* are derived without computing the intermediate *EDPs* and *DS*. The proposed method for constructing these loss surfaces is to discretize the empirically generated loss distributions by their decile and construct a linear interpolant function in between them.

The loss distributions considered in this study (financial losses and recovery times) are generated using the *FEMA P-58* and *REDi* methods, as illustrated in Fig. 1b). The collapse probability can be determined from a *FEMAP-154* Score [8]. Given an input seismic intensity, if collapse occurs, the replacement costs and time are assigned as the financial loss and recovery times. If collapse does not occur, the *FEMA P-58* and *REDi* procedures are followed to determine the financial losses and the recovery times. Once the loss distributions are generated for the key buildings, they are assigned to each building in the portfolio being represented by that archetype (due to similar structural systems, floor area, fundamental period, and structure deficiencies. The assigned loss distributions are then called in each realization to produce a loss value (financial or otherwise) using Monte Carlo sampling of the seismic intensity. In this step, different building-specific loss quantities of interest are determined independently. In addition to financial loss and recovery time, other loss distributions for other building-specific performance metrics derived from these loss quantities.

3. Assessment of Makati and Quezon City Public School Building Stock

3.1 Introduction

To investigate the seismic resilience of a building stock to *MM* seismic hazard, the *MC* and *QC* Disaster Risk Reduction Management Offices (*DRRMOs*) were engaged by the authors in 2017. High-level inventories were assembled consisting of 1,028 buildings (96 buildings across 41 campuses in *MC* and 932 buildings across 142 campuses in *QC*, as of 2017). The 2013 *QC* building inventory required updating with the latest (2016-2017) site development plans of the 142 campuses made available. Both inventories provided the buildings' names and locations, number of stories, and approximate floor areas. Specific detail about the structural systems, but the *QC* inventory classified buildings as "Concrete", "Semi-Concrete", "Steel", "Wooden", "Pre-fab", often indicating the materials being used for the walls and roofs. Architectural drawings of 55 buildings and structural drawings of 10 newer (1999-2009) buildings were provided by *MC* [15], and revealed the prevalent use of bonded post-tensioned-girder (*PT*) *RC-MRFs*. Structural drawings of modern modern (2011+) steel-*MRF* and *RC-MRF* buildings were provided by *QC* [16]. Earlier versions (2007-2012) of modern public school building drawing standards were made available by the Philippine Department of Education (*DepEd*) [17].

3.2 Structural Code Vintage Review

To break down the classification of structural systems, an analysis of National Building Code (*NBCP*) and National Structural Code of the Philippines (*NSCP*) [18] was made. *NBCP/NSCP* editions are derivatives of earlier versions of the Uniform Building Code (*UBC*) and *ACI-318* documents. With guidance from *UPC-ICE* [13], Wilfredo Lopez (former Department of Public Works & Highways, *DPWH*, Chief Structural Engineer) [19], and other studies [4;5], the pre-*NBCP*-1972, *NBCP*-1972/1981/1986, *NSCP*-1992, and *NSCP*-2001/2010/2015, were classified as "Pre-Code", "Low-Code", "Mid-Code", and "High-Code", respectively. These division mark significant changes in the seismic detailing requirements. Reconnaissance of post-1990 Luzon Earthquake revealed the lack of implementation of the limited seismic detailing requirements for *RC-MRFs* stipulated in Low-Code editions [19]. This gave rise to *NSCP* 1992, which contained a separate (and clearer) section on seismic detailing of *RC-MRFs* using probable moment capacities (M_{pr}) and more stringent shear reinforcement spacing to ensure ductile yielding mechanisms. A parametric study made apparent significant increases in design base shear base of 50-125% between *NSCP*-1992 and -2001, applicable to low-/mid-rise *RC-MRFs* in *MC* and *QC*. Thus, a "Mid-Code" was added to address this, despite the *UPD-ICE* not differing between "Mid-Code", and "High-Code". A 2-year lag period



between a school building's construction start date and the corresponding *NSCP* edition implemented in its design is assumed [19].

3.3 Rapid visual screening and archetype distributions

To enhance the provided information on the building stock, an *RVS* was conducted in early-2018 on 53 out of the 96 Makati public school buildings (55%) and 129 out of 932 buildings, with the assistance of *DepEd*. *FEMAP-154* Level 1 and 2 Scoring was performed to identify typical structural systems in use and possible structural deficiencies, horizontal & vertical irregularities, and possible pounding issues.

Low- (*L*, 1-2 stories), mid- (*M*, 3-6 stories), and high-rise (*H*, 10-11 stories) *RC-MRFs*, equivalent to *HAZUS/UPD-ICE* "*C1-L*" and "*C1-M*" typologies, were found to be the primary typology in *MC* (97% of buildings/99% by floor area). Most *MC* schools built post-1993 are believed to be *PT-RC-MRFs* or *PT-C1* [15]. This may be the case with earlier buildings, depending on the column spacing in longitudinal bays being greater than 5m and the relative depths of girders to such spans. *RC-shearwalls* were identified in 2 low-rise buildings (*UPD-ICE* "*C4-L*") through the rebar scanning of 5 possible candidates, with the assistance of engineers from SY². Structural drawings of one mid-rise building with *PT-girders* and *RC-shearwalls* were available.

In *QC*, 68.9% (73% by floor area) of buildings were found to be *C1-L* or *C1-M*. A number of buildings resembled the 1994 *DPWH* [20] school standards (low-/mid-rise *RC-frames* with *RC-shearwalls*, *C4-L/C4-M*), however it is believed that only a few of these archetypes were constructed in *MM* [19]. Significant contributions were provided by mid-rise steel-MRFs (*S1-M*, 7.8% by number of buildings & 16.3% by floor area) with concrete-encased columns. Buildings labelled as "Pre-fab" in the inventory were seen to be 1-storey light steel frames (*UPD-ICE* "*S3-L*"), reinforced/un-reinforced masonry using concrete hollow blocks (*CHB*), or *RC-MRFs* (possibly pre-cast, *PC2-L*). "Makeshift" buildings made from plywood, tarpaulin, or galvanized iron (G.I.) sheet walls/roofs nailed to wood frames, were also observed and correspond to the *UPD-ICE* "*N-L*" typology [13]. "Wooden" buildings were equivalent to *UPD-ICE* "*W1*" wood-frame typology. Buildings labelled as "Semi-Concrete" in the inventory appeared to be *C1-L* with wooden partitions or flooring, while one building was a 1 wooden-storey atop a 1-storey *RC-MRF*, equivalent to the *UPD-ICE* "*CWS-L*". These observations in *QC* were consistent with 2010-2011 *RVS* conducted by the *DPWH* [19] on 816 school buildings in *MM* (including 100 in *QC* and 7 in *MC*). Gilani & Miyamoto [5] classify all *MM* school buildings as *C1-L* and *C1-M*. The most probable archetype distributions are illustrated in Fig. 2, in which insignificant number of Pre-Code, unknown, and other minor building typologies are excluded from *QC*.

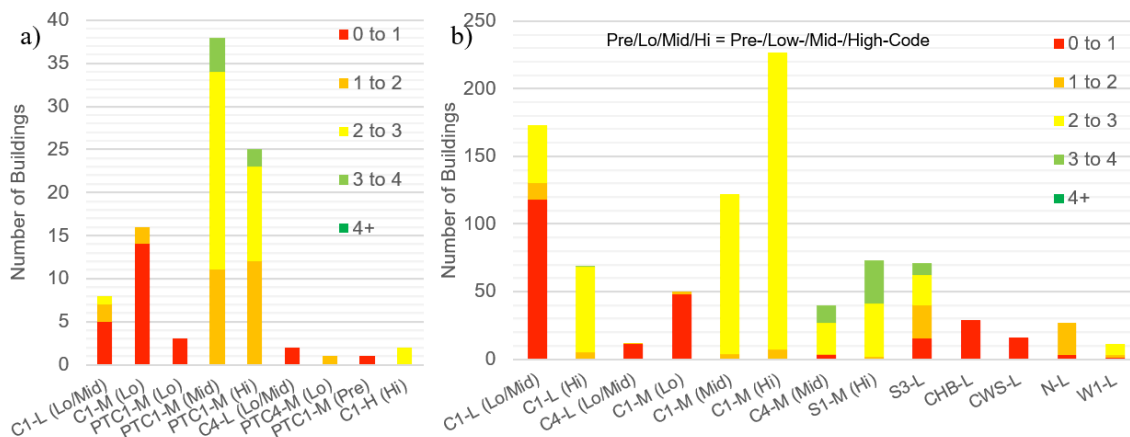


Fig. 2 – FEMAP-154 score & archetype distribution in a) Makati City; b) Quezon City

The balance of the *MC* and *QC* inventories had to be categorized based on the *RVS* observations and the aforementioned previous studies. Due to uncertainties in accurately identifying the structural systems of these buildings, two possible archetypes were assigned, with a greater certainty for *MC* buildings. The names



and building type provided in the *QC* inventory were indicative of the funding source (ie. *DepEd/DPWH* or *QC* politicians) and were often architecturally similar. Consequently, this is used to extrapolate the assigned archetypes of buildings that were not screened. Properties such as floor area, number of rooms, room size, and assigned student population (school enrolment divided by proportion of total school floor area) had to be approximated from other buildings with similar names/code vintages when entries were missing. Plan shapes, and separations/merging of building entries with/without seismic gaps, were encoded from site development plans and *RVS* observations (and architectural drawings for *MC*). *FEMAP-154* Scores were also extrapolated in a similar fashion. Buildings no longer the *QC* site development plans were marked as demolished, amounting to 139 buildings in a 5-year span. An early survey on the structural assessment of 23 *QC* public schools conducted in 2017 [16] also revealed that all pre-code buildings are ear-marked for demolition. *MC* is also in the process of replacing its older 2-/3-storey buildings [15].

4. Defining Key Building Archetypes

As a preliminary assessment of the building portfolio seismic resilience, 4 key *RC-MRF* archetypes were modeled: *C1-L* (High-Code), *C1-M* (Low-Code), *C1-M* (Mid-Code), and *C1-M* (High-Code), representing 468 or 50% (59% by floor area) of the total 932 *QC* buildings. Until detailed models of *PT-RC-MRFs* for *MC* are complete, the 4 *RC-MRF* archetypes provide a substitute, representing 83 or 85% (76% by floor area) of the total 96 *MC* buildings. Future works will ideally incorporate models for *PTC1-M* (Mid-/High-Code), *C1-L* (Low-/Mid-Code), high-rise *C1-H* (High-Code), *S1-M* (High-Code).

4.1 Assessment of available structural drawings and Re-designs

DepEd [18] structural/architectural drawings were used in defining the High-Code *C1-L* (2-Storey, 6-Classroom) and *C1-M* (4-Storey, 8-Classroom) archetypes as illustrated in Fig. 3. The Low- and Mid-Code *C1-M* archetype definitions required a re-design of a typical 3-storey, 12-Classroom *RC-MRF* in *QC*, following the requirements of *NBCP* 1972/1982 and *NSCP* 1992, respectively. Rough member sizes, plan and section dimensions were taken from *RVS* observations. Structural drawings of Low-Code *C4-L*, *C4-M*, and *C1-L* buildings were provided by the *DPWH* [20] in addition to guidance on typical design practice [19]. The High-Code buildings used one-/two-way slabs supported on beams or girders on all sides. The re-designed *C1-M* (Low-/Mid-Code) building typically made use of cast-in-place (or prefabricated) one-way ribbed *RC* slabs. Existing structural drawings indicate Live Loads of 2kPa for classrooms, 2.4kPa for restrooms, and 4.8 (Low-/Mid-Code) or 3.8kPa (High-Code) for hallways and stairs. Super-imposed dead loads come from the 4" or 6" *CHB* interior and exterior walls. High- and Mid-Code buildings used a steel roof-truss system supporting a suspended ceiling on lumber joists above the top floor, while Low-Code buildings had a similar timber truss-system. Isolated/combined footings are used to support the structures with footing tie-beams/grade-beams were used to ensure a fixed column base condition. *C1-M* (High-Code) uses a specified concrete strength (f'_c) of 27.6MPa, longitudinal reinforcement with yield strength (f_y) of 414MPa, and transverse reinforcement ($f_{y,v}$) of 276MPa. *C1-L* (High-Code) uses $f'_c = 21\text{MPa}$ & $f_y = f_{y,v} = 276\text{MPa}$, while *C1-M* (Low- & Mid-Code) use $f'_c = 21\text{MPa}$, $f_y = f_{y,v} = 276\text{MPa}$, & $f_{y,v} = 226\text{MPa}$. The use of deformed reinforcement is consistently specified through all the gathered structural drawings.

Design seismic base-shears for the Low- and Mid-Code archetypes were 1410 kN and 910kN, respectively, resulting in more longitudinal reinforcement in the Low-Code building without the level of ductility provided in the Mid-Code building. A simplified portal-frame lateral load analysis was performed considering 5% accidental eccentricities. Critical frames were designed according to the *NSCP* for combined gravity and seismic loads. *C1-M* (Mid-Code) followed typical modern ductile detailing practice, using M_{pr} for probable seismic shears, strong-column-weak-beam checks, joint shear checks, and stringent *MRF* column and beam transverse reinforcement spacing. *C1-M* (Low-Code) used minor provisions of *NBCP*-1972/1982, in which confinement reinforcement was also provided in plastic hinge regions of columns and through joints. Less stringent tie-spacing at the column mid-height resulted in 2 sets of $\phi 10\text{mm}$ spaced at 150-175mm compared to 2 sets of $\phi 12\text{mm}$ at 120-150mm for similar-sized columns in the Mid-Code



equivalent. Similarly, Low-Code beam stirrups were $\phi 10\text{mm}$ at similar spacings/sizes to the Mid-Code beam with $\phi 12\text{mm}$ stirrups.

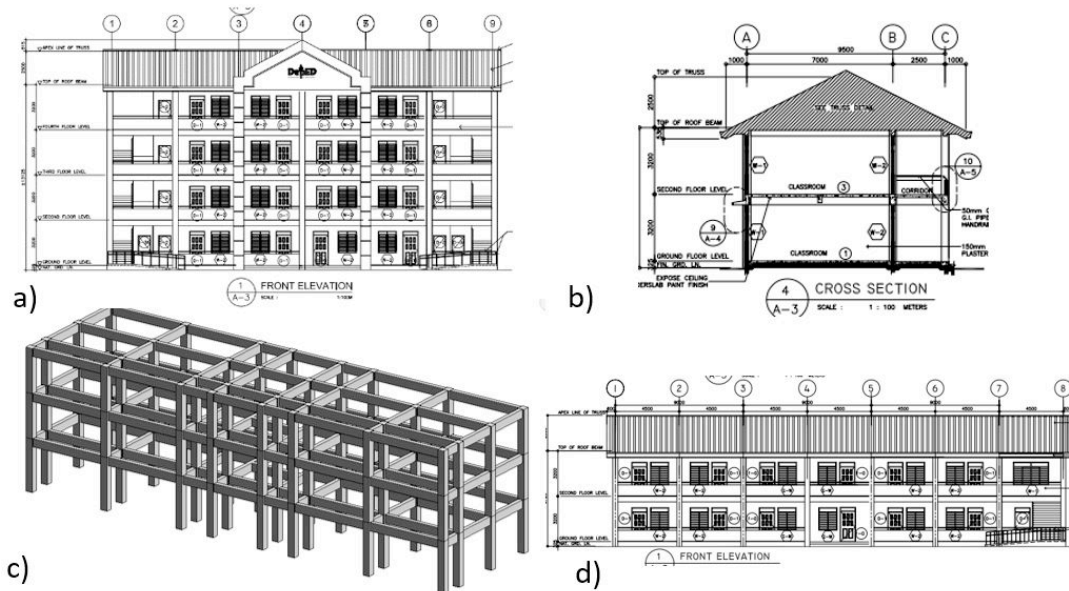


Fig. 3 – a, b, & d) *DepEd* C1-M and C1-L (High-Code) architectural drawings [18]; c) Revit model of C1-M (Low-/Mid-Code) re-design

Evidence from past earthquakes in the Philippines has shown that Pre- and Low-Code *RC-MRFs* (*CI-L*, *CI-M*, *CI-H*) typically experienced severe damage to columns, including diagonal shear cracks or “shortening” (compression failure), as a result of tie-spacing deficiencies or lack of 135° hooks. This led to “pancaking” or complete collapse of soft-storeys in some cases [19]. Modeling strategies for the non-ductile C1-M (Low-Code) are aimed at capturing this response.

4.3 Non-linear modeling of key building archetypes

The *ASCE41* [21] Tier 3 seismic evaluation methodology was followed in developing non-linear models of the 4 *RC-MRFs* with additional guidance from *NIST* [22]. Expected rebar yield ($f_{y,e}$) was taken as $1.2f_y$, while expected unconfined concrete compressive ($f'_{c,e}$) is taken as $1.1f'_c$ to account for substandard construction quality control. Linear elastic models were first developed in *SAP2000* while appropriately accounting for cracked sections and increased beam bending stiffness due to contribution of slabs [22]. Models with their assigned loads, nodal masses, and section properties were exported to *PERFORM-3D*, where non-linear behavior of elements were defined.

The *RC-MRF* columns and beams were modeled with lumped plasticity elements (*FEMA-Column/Beam*) in *PERFORM-3D*, which use an elastic *RC* beam-column line element bounded by zero-length chord-rotation plastic hinges at the column faces. The backbone and acceptance criteria are defined with plastic rotations, θ_p and θ_{pc} , specified in *ASCE41* for flexure-controlled beams with conforming transverse reinforcement (Mid-/High-Code), for shear-controlled beams (Low-Code beams with expected shear failure), and for columns not controlled by inadequate slicing or development.

Non-linear shear behaviour was defined for the *CI-M* (Low-Code) archetype due to the deficiencies implemented in its design, in which shear hinges are placed at the mid-span of *MRF* beams and columns. Shear hinges were defined [23] appropriately, which are un-coupled from the axial-flexural or flexural response of columns and beams was provided.

CHB material properties examined in the Philippines [19;24] used with *ASCE41* in modeling the infill walls. 6” *CHB* walls were implemented in *PERFORM* using equivalent “Inelastic Concrete Strut”



components, defined by converting the wall shear strength into a compressive-strut stress and the inter-storey drift-based *ASCE41* backbone into equivalent strains. The walls were eccentrically connected on the columns in the Low-Code model, to simulate increased column shear demands due to infills. No significant impacts of infill were found, except increases in all initial buildings' stiffness in the transverse direction.

The *RC* slabs were not modeled explicitly, and rigid diaphragms were set at these stories. The steel roof trusses, purlins, and $\varnothing 12$ to 16mm bar diagonal bracing in the High- and Mid-Code buildings were modeled in *SAP2000*. Equivalent in-plane shear stiffnesses were calculated for bays with and without cross-bracing and modeled in *PERFORM* with "Linear Elastic Infill Panel" components. Timber trusses were ignored. Columns were fixed at the base, as modeling of foundations is deemed to be insignificant due to the use of footing tie-beams. Stiff joints were modeled by using default end-zone elements in the MRF beams and columns with the stiffness of the panel zone being 10 times that of the frames. This was considered appropriate considering the confinement level provided even in the Low-Code archetype. SSI effects were neglected for this study. Rayleigh damping is specified for the model such that the damping ratio at 0.25 and 1.5 times the first fundamental mode period (T_1) is 2.5%. P-Delta Effects were included in the models. Collapse indicators assumed for the models include column plastic-hinge plastic rotations reaching *ASCE41* Collapse Prevention (CP) level, inter-storey drifts (*IDR*) exceeding 5%, and shear-hinges in the Low-Code model reaching the post-peak residual strength.

5. Seismic Hazard Definition

5.1 Philippine Earthquake Model and spatial distribution of sites

The most up-to-date probabilistic seismic hazard assessment (*PSHA*) for the Philippines was developed by *GEM & PHIVOLCS* [1], and shows that the *MM* hazard is largely governed by the *EVF & WVF* (distances $< 25\text{km}$ and M_w 6.5-7.75) with a second cluster of non-zero probability of exceedance attributed to the Manila Trench (subduction interface & subcrustal zone) a distances of 100 to 150km (M_w approaching 8). *GEM* [25] provided the authors with mean spectral acceleration (S_a) values at periods, $T = \{0, 2s\}$ and for return periods, $T_R = \{75\text{-year}, 175\text{-year}, 475\text{-year}, 975\text{-year}, 2475\text{-year}\}$, on a reference average shear-wave velocity ($V_{s,30}$) of 760m/s. Site-class (soil) conditions were assumed at each school location from an earlier version of the Philippine Earthquake Model [26], as illustrated in Fig. 4. Regions declared as Soil B ($V_{s,30} = 760\text{-}1500\text{m/s}$) did not align with the hybrid site-class model developed for the *GMMA-RAP* [3] and appear to have Soil C ($V_{s,30} = 360\text{-}760\text{m/s}$) values in the region. Thus, school campuses were instead grouped into Soil D ($V_{s,30} = 180\text{-}360\text{m/s}$), Soil "C1" ($V_{s,30} = 360\text{-}760\text{m/s}$ & $\leq 5\text{km}$ from the *WVF*) and Soil "C2" ($V_{s,30} = 360\text{-}760\text{m/s}$ & $> 5\text{km}$ from the *WVF*). [1] used the *BA08* [27] GMPE to represent the median S_a of shallow crustal faults, and thus *BA08* site-amplification factors applied to the S_a on reference $V_{s,30}$. Median (of each site per soil group) target spectral acceleration (TS_a) curves were defined.

5.2 Average directivity amplification and definition of maximum and minimum direction spectra

NIST [29] guidelines on ground-motion selection were followed due to a lack of in-depth recommendations in the latest *NSCP*. There is an apparent need to account for average directivity effects or other near-fault phenomena causing significant velocity time-history pulses, while selecting appropriate global seed *GMs* to match the shape of the TS_a . The *SB13* [29] model for average directivity amplification ($\mu_{ln(AMP|M,R,T)}$) for vertical strike-slip ruptures is chosen, as it requires minimal input values of magnitude (M) closest source-to-site distance ($R = R_{rup}$), and selected periods (T). The mean of $\mu_{ln(AMP|M,R,T)}$ calculated for a range of T , the R of each site from the *WVF*, and for $M = \{6.2, 6.5, 7, 7.2, 7.5\}$ corresponding to 5 selected intensities, based on the magnitude frequency distribution described by [1].

Preliminary seed *GMs* that were selected from the *NGA-West2* database [30] and amplitude-scaled led to excessive required scale-factors, without being able to match the spectral shape of the TS_a . The orientation of input *GMs* to a structural model generally needs to be consistent with strike-normal and strike-parallel, for near-fault sites [28].

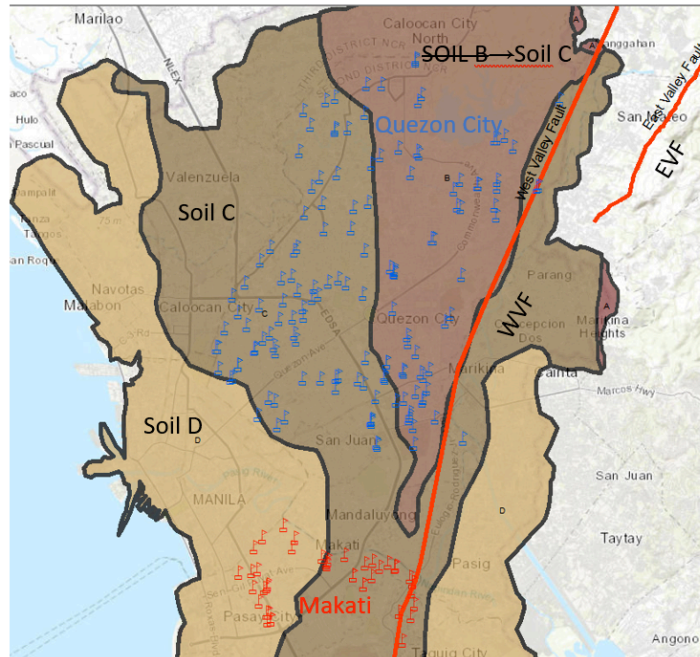


Fig. 4 – Spatial distribution of Makati and QC campuses with WVF, EVF, and soil classification

To address these issues, the bi-directional time-domain spectral-matching script developed *RspMatchBi* [31] was used. Input TS_a are required for the spectral matching of seed *GMs*, which define major- and minor-axis S_a demand (target maximum and minimum direction spectra, $TS_{a,MaxDir}$ & $TS_{a,MinDir}$, respectively) resulting from the polarization of near-fault *GMs*. The empirical *SB13* [29] model for *GM* directionality is implemented to convert geomean TS_a values to $TS_{a,MaxDir}$ using the developed $S_{a,RotD100}/S_{a,RotD50}$ ratios, or the ratio of 100th percentile rotated S_a of an orthogonal acceleration time-history to the 50th percentile value. Geomean period-independent response spectra ($S_{a,GMRot150}$) used in NGA-West GMPEs and used by [1] are only slightly different (6 to 7%) to $S_{a,RotD50}$ [32]. $TS_{a,MinDir}$ is derived using mean η values proposed by [33] and for the purpose of this study correspond to the $S_{a,RotD0}$, which is not necessarily perpendicular to the $S_{a,RotD100}$.

5.3 Ground-motion selection and spectral matching

9 pulse-like and 1 non-pulse seed shallow-crustal *GM* pairs are selected from [30], with the 2475-year $TS_{a,MaxDir}$ per soil group corresponding to the median intensity at those sites. Strike-slip and reverse fault mechanisms, the appropriate $V_{s,30}$ group, and $R_{jb}=\{0,35km\}$, for a T range of $\{0.2T_{n,min}, 3T_{n,max}\}$ of the 4 models. 1 subduction *GM* record pair (per *Soil C* or *Soil D*) was selected from the 2010 Maule, Chile Earthquake [34]. Sub-crustal contributions are ignored for this study due to limited disaggregation information. The spectral matching procedure outlined by [35] was adapted to consider and preserve velocity pulses during spectral matching, to develop *GM* suites at each intensity and for each group of sites. The *SB14* [36] algorithm to identify and extract velocity pulses in orthogonal *GM* record pairs was implemented to process the selected pulse-like *GMs* for spectral matching. *RotDSpectro* script [37] was used to calculate $S_{a,RotD100}$ of the subduction *GM* records and $S_{a,RotD0}$ and $S_{a,RotD50}$ of all records. Pulse-like *GMs* were rotated to the direction of the largest identified pulse, the velocity pulse was extracted leaving a residual acceleration-time history, $a_{max,residual}(t)$, in the maximum direction component and acceleration time-history perpendicular to $a_{max,residual}(t)$ is declared as the minimum direction component, $a_{min}(t)$. Non-pulse *GMs* relied on a similar process except the maximum direction, $a_{max}(t)$, was defined with the mode of $S_{a,RotD100}$ rotation angles at a range of $T=\{0.5,1s\}$. *RSPMatchBi* was used to perform broad-band bi-directional spectral matching of the $a_{max,residual}(t)$ or $a_{max}(t)$, and $a_{min}(t)$ pairs to the $TS_{a,MaxDir}$ and $TS_{a,MinDir}$. The initially extracted velocity pulses were then added back to $a_{max,residual}(t)$. Measures of change introduced by spectral matching were checked for each record pair in all *GM* suites following [28] and the pulse-like nature of the final *GM* were also checked.



6. Portfolio Loss Estimation

6.1 Building-Specific Seismic Performance Assessment

15 sets of *GMs* (3 soil group x 5 intensities) totaling 165 time-history simulations were run for each of the modeled archetypes. *EDPs* of inter-storey drift ratio (*IDR*), residual storey drift ratio (*RDR*), peak floor accelerations (*PFA*), and peak floor velocity (*PFV*) were extracted from *NLDTH* results and imported.

An in-house software was used to generate the loss-distributions for each modeled archetype (4 archetypes x 3 soil groups) using 2000 Monte Carlo realizations. A formulation for building replacement value was determined from “Contract Amount” values of buildings (built 2010+) for the 4-archetypes and all the buildings in the portfolio they represent. Since *FEMAP-58* component losses are based on North American (*NA*) experience, an equivalent North American building replacement value (USD2,470/m²) was assigned [39] to each building. For example, the Philippine replacement cost of the 915m² *CI-M* (Low-Code) is US\$0.28m with an equivalent *NA* cost of US\$2.26m and resulting replacement time of 402 days (using $e^{0.31\ln(NA\ value)+1.46}$). Individual (and minimal) non-structural contents were assigned per storey to each building, and consisted of *CHB* infills walls, windows, book shelves, minimal plumbing, and suspended ceilings over the top storey. An approximation had to be made for the windows to be replaced by curtain walls, *CHB* represented by “ordinary reinforced masonry walls” (reduced by a subjective factor of 0.4 as *CHB* walls are non-structural), and structural contents (beam-columns) to be factored down for smaller framing sizes based on industry experience. The *P58* population model and default fatality rates for Middle Schools are applied to the assigned # students per building.

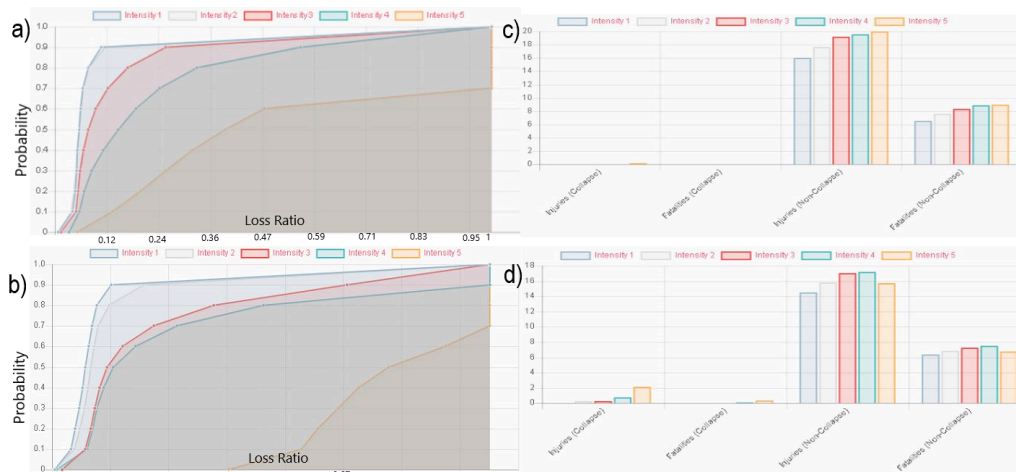


Fig. 5 – Loss Ratio & Casualties for a,b) C1-M (High-Code) & c,d) C1-M (Low-Code)

The collapse probability was determined by *FEMAP-154* scoring, such as with *CI-M* (Low-Code) scores of 1 on Soil D & C1 and 1.2 on Soil C2, relating to a probability of 0.07 and 0.1, respectively leading to median collapse S_a of 3, 2.6, and 2.2g, respectively, assuming a dispersion of 0.6. Resulting losses of the building on Soil D for an *MCE* (2475-year) event is primarily attributed to beam-columns and *CHB* walls, summing up to US\$0.11m (when results are scaled back down to Philippine values). The estimated re-occupancy under a *DBE* (475-year) is just under 250 days and 350 under an *MCE* event. Downtime estimates were also using *NA* values and calibration from past Philippine earthquakes is required. Fig. 5 illustrates expected loss ratios and casualties for C1-M (High-/Low-Code). Excessive drifts due to shear-failure and collapses under some records of 975-/2475-year intensities.

6.2 Portfolio Loss Estimation

The reduced 551-building portfolio, with a total replacement value of about USD289m (Philippine value) and population of around 225,000 is assessed under the most probable event [3] from the *WVF*, an M_w 6.5, using 500 Monte Carlo realizations per building. The appropriate *GMPEs* set out for crustal faults and



subduction mega-thrust sources are selected from [1] and a spatial correlation [39] is assumed. A preliminary median portfolio loss of US\$40m and total casualties (injuries & fatalities, collapse & non-collapse) of 28,400 people, the results of which are illustrated in Fig. 6.

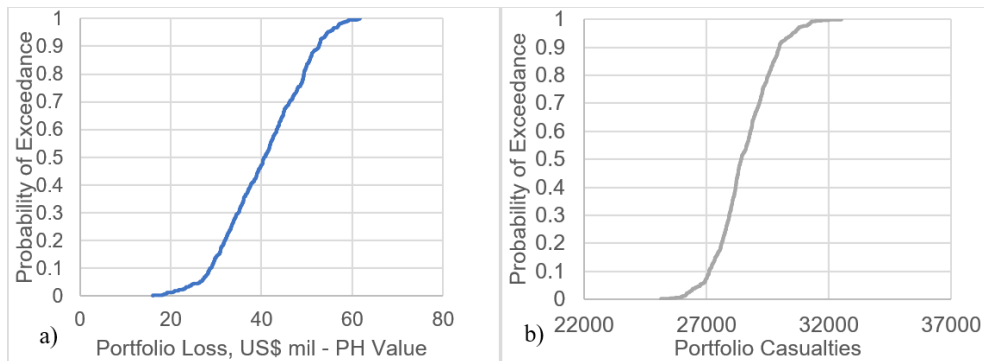


Fig. 6 – Probability of exceedance of portfolio casualties and total loss (NA values)

7. Conclusion

An integrated methodology with building-specific risk and downtime assessments applied to the regional seismic risk and performance assessment of a multi-building portfolio, is presented. The methodology extends decile-based linear-interpolant building-specific vulnerabilities to general financial loss (implementing *P58*) and recovery-time (with *REDi*) distribution functions in a rapid manner. The methodology is applied to a 551-building *RC-MRF* portfolio across two cities in Metro Manila, which involved screening of building to group and select key structural archetypes for the development of detailed non-linear models. The *MM* seismic hazard is defined by selecting and bi-directional spectral-matching *GM* suites at 5 intensities, while considering near-fault effects and the latest Philippine *PSHA*. Building-specific vulnerabilities are developed and assigned to each building in the portfolio to assess the overall portfolio losses under the most probable fault-scenario from the *WVF*.

8. Disclaimer & Acknowledgements

These works are still subject to review and further refinement. The authors would like to thank all participating departments of Makati (*DRRMO, GSD, UDD, DEPW*) and Quezon City (*DRRMO, CAD, ED*); the Philippine *DepEd, DPWH, PHIVOLCS*, and *DILG*. The support of Engr. Lopez and *EMI*, and the technical assistance by Mr. Al Roben Adriane Goh from Kinetica are greatly appreciated.

9. References

- [1] Peñarubia, H., Johnson, K., Styron, R., Bacolcol, T., Sevilla, W., Perez, J., . . . Allen, T. (2019). Probabilistic Seismic Hazard Analysis model for the Philippines. *Earthquake Spectra*. In press.
- [2] NDRRMC. (2020). *NDRRMC Update: SitRep No. 15*. Quezon City, Philippines: Republic of the Philippines National Disaster Risk Reduction and Management Council.
- [3] Allen, T., Ryu, H., Bautista, B., Bautista, L. M., Narag, I., Sevilla, W., . . . Bonita, J. (2014). *GMMA-RAP*. PHIVOLCS and Geoscience Australia. Manila, Philippines.
- [4] JICA et al. (2004). *MMEIRS*. JICA; MMDA; PHIVOLCS; Pacific Consultants International; OYO International Corporation; Pasco Corporation, Manila, Philippines.
- [5] Gilani, A. S., & Miyamoto, H. K. (2017). Seismic Risk Reduction Program for School and Hospital Buildings in Metro Manila, Philippines. *16WCEE Proceedings*. Santiago, Chile.
- [6] FEMA. (2012). *HAZUS-MH 2.1 - Multi-hazard Loss Estimation Methodology - Earthquake Model*. Washington, D.C.
- [7] FEMA. (2018). *Seismic Performance Assessment of Buildings*, FEMA P-58 3rd ed. ATC for FEMA, Washington, D.C.
- [8] USRC. (2015). *USRC Building Rating System - Implementation Guide*. U.S. Resiliency Council.
- [9] Arup. (2017). *UBC Seismic Resilience Study - Seismic Risk Assessment and Recommended Strategy (Issue 2)*.



- [10] Almufti, I., & Willford, M. (2013). REDi Rating System - Resilience-based Earthquake Design Initiative for the Next Generation of Buildings. Arup.
- [11] ATC. (2015). *FEMA P-154 Rapid Visual Screening of Buildings*, 3rd ed. ATC for FEMA, Washington, D.C.
- [12] Guo, J., Jeswani, K., Christopoulos, C. (2018). An Integrated Methodology for Urban Seismic Resilience Planning. 16ECEEE Proceedings. Thessaloniki, Greece.
- [13] Tingatinga, E.A.J., Pacheco, B.M., Hernandez Jr., J.Y., Pascua, M.C., Tan, L.R.E., ..., Germar, F.J. Development of seismic vulnerability curves of key building types in the Philippines. *2019PCEE Proceedings*. Auckland, New Zealand.
- [14] Jalayer F, Cornell CA (2009). Alternative non-linear demand estimation methods for probability-based seismic assessments." *Earthquake Engineering & Structural Dynamics*, 38, pp.951–972.
- [15] Makati City –Disaster Risk Reduction Management Office (DRRMO), Urban Development Department (UDD), General Services Department (GSD), Department of Engineering & Public Works (DEPW). (2017-2018). Personal communication.
- [16] Quezon City – Disaster Risk Reduction Office (DRRMO), Office of the City Architect, and Office of the City Engineer. 2017-2018. Personal communication.
- [17] Department of Education (DepEd) – Makati Division Office, Quezon City Division Office, Disaster Risk Reduction and Management Service (DRRMS), Educational Facilities Division. 2017-2019. Personal communication.
- [18] ASEP. (1972-2016). *National Building Code/Structural Code (NBCP/NSCP) 1st to 7th Edition*. Quezon City, Philippines: Association of Structural Engineers of the Philippines, Inc. (ASEP).
- [19] Wilfredo Lopez. 2017-2020. Personal communication.
- [20] Department of Public Works & Highways, Bureau of Design. 2017-2018. Personal communication.
- [21] ASCE/SEI. (2017). *ASCE/SEI 41-17*. Structural Engineering Institute (SEI). Reston, VA. American Society of Civil Engineers.
- [22] ATC/NIST. (2017). *Guidelines for Nonlinear Structural Analysis for Design of Building*. Gaithersburg, MD: ATC NIST.
- [23] Zimos, D.K., Mergos, P.E., Kappos, A.J. 2018. Modelling of R/C members accounting for localisation: Hysteretic shear model. *Earthquake Engng. Struct. Dyn.* 2018;47:1722–1741.
- [24] Mendoza Jr., R. P., Cruz, E. S., & Senoro, D. B. (2011). Modeling of CHB Masonry for Seismic Analysis of Low-Rise Reinforced Concrete Frames. *37th National Convention PICE*. Cagayan de Oro, PH.
- [25] Richard Styron. 2019. Personal communication
- [26] PHIVOLCS. (2017). *The Philippine Earthquake Model*. Philippine Institute of Volcanology and Seismology (PHIVOLCS). Manila, Philippines.
- [27] Boore, D., & Atkinson, G. (2008). Ground-Motion Prediction Equations *Earthquake Spectra*, 24(1), 99-138. doi:10.1193/1.2830434
- [28] NIST. (2011). *NIST GCR 11-917-15 - Selecting and Scaling Earthquake Ground Motions for Performing Response-History Analyses*. Gaithersburg, MD. National Institute of Standards and Technology (NIST).
- [29] Shahi, S. K., & Baker, J. W. (2013). *A Probabilistic Framework to Include the Effects of Near-Fault Directivity in Seismic Hazard Assessment*. Berkeley, CA. Pacific Earthquake Engineering Research Institute.
- [30] PEER. (2013). *NGA-West2 Ground Motion Database*. Retrieved 2019, from PEER Ground Motion Database: <https://ngawest2.berkeley.edu/>
- [31] Grant, D. N. (2011). Response Spectral Matching of Two Horizontal Ground-Motion Components. *Journal of Structural Engineering*, 137(3), 289-297. doi:10.1061/(ASCE)ST.1943-541X.0000227
- [32] Boore, D. M. (2010). Orientation-Independent, Nongeometric-Mean Measures of Seismic Intensity from Two Horizontal Components of Motion. *Bull. of the Seis. Soc. of America*, 100(4), 1830-1835. doi:10.1785/0120090400
- [33] Hong, H., & Goda, K. (2007). Orientation-Dependent Ground-Motion Measure for Seismic-Hazard Assessment. *Bulletin of the Seismological Society of America*, 97(5), 1525-1538. doi:10.1785/0120060194
- [34] UCS. (2010). *Terremotos de Chile / Earthquake of Chile*. Retrieved 2019, from RENADIC: <http://terremotos.ing.uchile.cl/registros/164>
- [35] Grant, D. N. (2012). Preservation of Velocity Pulses in Response Spectral Matching. *Proceedings of The 15th World Conference on Earthquake Engineering*. Lisboa, Portugal.
- [36] Shahi, S. K., & Baker, J. W. (2014). An Efficient Algorithm to Identify Strong-Velocity Pulses in Multicomponent Ground Motions. *Bulletin of the Seismological Society of America*, 104(5), 2456-2466. doi:10.1785/0120130191
- [37] Kong, C., Thangappa, R. 2019. Personal communication
- [38] Altus Group. 2018. Canadian Cost Guide. Retrieved 2020, <http://creston.ca/DocumentCenter/View/1957/Altus-2018-Construction-Cost-Guide-web-1>
- [39] Loth,C., Baker, J.W. (2011). A spatial cross-correlation model of spectral accelerations at multiple periods. *Earthquake Engineering and Structural Dynamics*. 42(3): 397-417.